



#### AUTHORS:

Glynn K. Pindihama<sup>1</sup>   
Mugera W. Gitari<sup>1,2</sup>   
Rabelani Mudzielwana<sup>1</sup>   
Ntakadzeni E. Madala<sup>3</sup>

#### AFFILIATIONS:

<sup>1</sup>Environmental Remediation and Nano Sciences Research Group, Department of Geography and Environmental Sciences, Technical University of Science, Engineering and Agriculture, University of Venda, Thohoyandou, South Africa

<sup>2</sup>Department of Chemical Sciences and Technology, School of Chemistry and Material Sciences, Technical University of Kenya, Nairobi, Kenya

<sup>3</sup>Department of Biochemistry and Microbiology, Faculty of Science, Engineering and Agriculture, University of Venda, Thohoyandou, South Africa

#### CORRESPONDENCE TO:

Glynn Pindihama

#### EMAIL:

gpindihama@gmail.com

#### DATES:

Received: 15 Sep. 2022

Revised: 16 Mar. 2023

Accepted: 30 Apr. 2023

Published: 28 Sep. 2023

#### HOW TO CITE:

Pindihama GK, Gitari MW, Mudzielwana R, Madala NE. Development of a chitosan-multi-walled carbon nanotubes composite for application in solid-phase adsorption toxin tracking of microcystins. *S Afr J Sci.* 2023;119(9/10), Art. #14786. <https://doi.org/10.17159/sajs.2023/14786>

#### ARTICLE INCLUDES:

- Peer review  
 Supplementary material

#### DATA AVAILABILITY:

- [Open data set](#)  
 All data included  
 On request from author(s)  
 Not available  
 Not applicable

#### EDITORS:

Priscilla Baker   
Amanda-Lee Manicum

#### KEYWORDS:

chitosan, multi-walled carbon nanotubes, solid-phase adsorption toxin tracking, microcystins

#### FUNDING:

Water Research Commission (K5/2972)

© 2023. The Author(s). Published under a Creative Commons Attribution Licence.

# Development of a chitosan-multi-walled carbon nanotubes composite for application in solid-phase adsorption toxin tracking of microcystins

Contamination of water and food with cyanotoxins poses human health risks, and hence the need for sensitive early warning tools to monitor these in water. A composite of glutaraldehyde-crosslinked chitosan and multi-walled carbon nanotubes (ChMWCNTs) was synthesised and tested for potential use as a solid-phase adsorption toxin tracking (SPATT) adsorbent for monitoring microcystins (MCs) in fresh water. The composite was characterised by Fourier transform infrared spectroscopy, Brunauer–Emmett–Teller theory and scanning electron microscopy. Batch adsorption experiments to assess the effect of contact time, adsorbent dosage and initial microcystin-LR (MC-LR) concentration were conducted. The composite was found to be efficient in adsorbing MC-LR, showing 97% removal and a maximum adsorption capacity of 4.639 µg/g under optimised conditions of 5 µg/L of MC-LR, adsorbent dose of 0.03 g/5 mL and 30 min contact time. The adsorption kinetics were better explained by a pseudo-second-order model, inferring chemisorption adsorption. The isotherm data better fitted the Langmuir isotherm model, thus inferring monolayer surface adsorption. For desorption, 100% methanol was the most effective, with an efficiency of 84.71%. The composite effectively adsorbed and desorbed three congeners of MCs (–LR, –RR and –YR) when tested in raw dam water, regardless of its lower maximum adsorption capacity compared to those of other adsorbents used for similar purposes.

#### Significance:

- Monitoring of microcystins is problematic in large reservoirs and rivers.
- Chitosan can be crosslinked and modified to enhance its adsorption properties.
- Composites of chitosan and carbon nanotubes efficiently adsorb and desorb microcystins.
- This study is possibly the first to apply a chitosan-based sorbent in solid-phase toxin tracking (SPATT) to be used as an early warning tool in passive monitoring of microcystins in water resources.

## Introduction

The global increase in incidents of toxin-producing cyanobacterial blooms has gained international attention in recent years. These increases have been attributed to a wide variety of environmental factors including nutrient pollution, increased temperature and salinity, many of which will likely be exacerbated by climate change.<sup>1,2</sup> Toxins produced by cyanobacteria (cyanotoxins) pose a significant risk for humans, livestock and wildlife as they can cause impairment and mortality.<sup>3</sup> Amongst the many types of cyanotoxins that have been documented, microcystins (MCs) are the most frequently occurring in the freshwater environment, and hence, have been widely investigated. Due to the chronic toxicity of MCs, the World Health Organization (WHO) set a provisional threshold of 1 µg/L for MC-LR concentration in drinking water<sup>4</sup> and a tolerable daily intake (TDI) of 0.04 µg MC-LR/kg body weight (BW) in food.<sup>1</sup> MC levels above this WHO threshold have been reported in South Africa, with levels in the range of 2 µg/L to 23.7 µg/L being reported in various water bodies in the country.<sup>5</sup>

Several countries have routine programmes to monitor these toxins and test possible contamination of food crops and fish. However, the drawback of the sampling and monitoring of these toxins in rivers and large water bodies is that their levels can vary rapidly.<sup>6</sup> To overcome the drawbacks of grab sampling, MacKenzie et al.<sup>7</sup> came up with the solid-phase adsorption toxin tracking (SPATT) technology, for possible use for the detection and early warning of the presence of cyanotoxins. SPATT involves suspending small bags containing adsorbent which accumulate toxins in the water body. The toxins can then be extracted and measured, providing information on extracellular toxins over an extended period.

Different sorbents have been used for SPATT, including the polymeric adsorbents Diaion® HP-20 to SEPABEADS-type resins for the accumulation of cyanobacterial toxins of different polarities.<sup>8</sup> Although passive sampling has been successfully used several times to monitor cyanotoxins using different bulk polymeric sorbents,<sup>8</sup> most of these sorbents are synthetic and relatively costly to buy. Studies on the characterisation and mechanism of SPATT resins for the adsorption of lipophilic and hydrophilic cyanotoxins are also limited.<sup>1</sup>

Recent studies, for example those of Gomez-Maldonado et al.<sup>9</sup> and Tran et al.<sup>10</sup>, have demonstrated that chitosan can be modified and be applied for the adsorption of MC-LR in water purification, but no studies have evaluated its use as a sorbent in the passive sampling of MCs in SPATT. Insertion of multi-walled carbon nanotubes (MWCNTs) into the chitosan hydrogel to form a chitosan-multi-walled carbon nanotube (ChMWCNT) composite was hypothesised to have the synergistic effect of improving the physical properties of chitosan and improve its adsorptive characteristics. Thus the aim of this work was to insert multi-walled carbon nanotubes into the chitosan





hydrogel structure and evaluate the subsequent effects on the formed composite material and its capabilities for MC adsorption and desorption for possible use in SPATT samplers.

## Materials and methods

### Chemicals and reagents

Analytical-reagent grade glutaraldehyde (GLA), acetic acid and powdered high molecular weight chitosan (Ch) were purchased from Rochelle Chemicals (Johannesburg, South Africa). Hydroxyl functionalised multi-walled carbon nanotubes (MWCNTs, purity: >98%, average diameter: 10–20 nm) were purchased from SabiNano (Pty) Ltd (Johannesburg, South Africa). Synthetic aromatic adsorbent Diaion® HP-20 resin was purchased from Rochelle Chemicals (Johannesburg, South Africa). De-ionised water from a Milli-Q water purification system (Merck-Millipore Ltd., Germany) of 18.2 MΩ/cm quality was used to prepare all the solutions. Microcystin-LR (MC-LR) standards, 0.5 mg films (Eurofins Scientific, USA) were purchased from ToxSolutions, Kits and Services (South Africa).

### Preparation of the ChMWCNT composite

Chitosan was crosslinked with GLA using ratios optimised by Gonçalves et al.<sup>11</sup> and chitosan-to-MWCNTs ratios applied by Alves et al.<sup>12</sup> In brief, chitosan (1 g) was dissolved in 50 mL of 1% v/v acetic acid. After the complete dissolution of chitosan, carbon nanotubes (CNT) (10 % wt) were added to the solution. Then, GLA (2% (v/v)) was used as a crosslinking agent and slowly added to the MWCNT-chitosan solution under mechanical stirring (50 revolutions per minute [rpm]) until it formed a gel. The formed hydrogel was freeze dried for 48 h at -48 °C under a constant vacuum of 44 μmHg (Telstar Lyoquest Freeze Dryer, Terrassa, Spain). The freeze-dried material was then ground to powder using a mortar and pestle, followed by sieving using a 250 μm sieve to get particles above 250 μm only (suitable to be used in SPATT bags).

### Characterisation

The Fourier transform infrared (FTIR) spectroscopy spectra of the chitosan (CH), glutaraldehyde-crosslinked chitosan (ChGLA) and the chitosan/MWCNT composite (ChMWCNT) were recorded using a Bruker Alpha-P FTIR spectrometer equipped with a diamond ATR window (Bruker Optik GmbH, Ettlingen, Germany). All spectra were recorded in the spectral range of 4000–400/cm with a resolution of 4/cm. Surface area measurements were conducted on a Micromeritics TriStar II 3020 Surface Area and Porosity Analyser (Norcross, Georgia, USA). The surface morphology of the samples was characterised using scanning electron microscopy (SEM; FEI Nova Nano SEM 230, USA).

### Adsorption and desorption studies

#### Optimisation of equilibration time

A 5 μg/L MC-LR solution was used to investigate the effect of contact time. The toxin solutions (5 mL) were placed in 15 mL glass centrifuge tubes with 0.01 g of the ChMWCNT composite and the mixture was shaken at 145 rpm (Stuart Reciprocating Shaker, SSL2, UK) for 5, 10, 15, 30 and 60 min at room temperature and immediately after, filtered through 0.22 μm pore membrane filters and the filtrate analysed for MCs using microcystins/nodularins (ADDA) enzyme-linked immunosorbent assay (ELISA) kits, EUROFINS (Kit Lot No: 19I1120: PN 520011, Eurofins Scientific, USA) and a SPECTROstar Nano Plate Reader (BMG LABTECH, 601-1106, Germany) for quantification.

#### Optimisation of dosage

A 5 μg/L of MC-LR (5 mL) and composite dosages 0.005 g; 0.01 g; 0.02 g; 0.03 g; 0.05 g and 0 g (control) were investigated by placing the composite in 15 mL glass centrifuge tubes and shaken at 145 rpm at room temperature for 30 min (as determined from the previous experiment on optimisation of equilibration time). Samples were then filtered through 0.22 μm pore membrane filters immediately after

agitation and the residual toxin levels in the supernatant determined as described in the section of optimisation of equilibration time.

### Adsorption and equilibrium studies

Adsorption experiments were conducted to investigate the adsorption isotherms at equilibrium and the kinetics. The effect of contact time and the kinetics studies were investigated by placing 0.03 g of ChMWCNT (the optimised unit dose) in 15 mL glass centrifuge tubes with 5 mL of 5 μg/L MC-LR solution. This was then followed by agitation for 5, 10, 15, 30 and 60 min; then it was filtered through 0.22-μm pore membrane filters, and the residual toxin levels in the supernatant were determined as described in the section of optimisation of equilibration time.

For the equilibrium study, 0.03 g of adsorbent was introduced into seven 15-mL centrifuge tubes with 5 mL of different MC-LR concentrations (within the range commonly found in South African water bodies<sup>5</sup>) (i.e. 2.5, 5, 7.5, 10, 15, 20, and 25 μg/L). The tubes were agitated for 30 min at room temperature. Afterwards, samples were filtered through 0.22 μm pore membrane filters immediately after agitation and the residual toxin levels in the supernatant were determined. Two isotherm models of Freundlich and Langmuir were employed to analyse the equilibrium data.

### Adsorption data modelling

The adsorption capacity ( $q_t$ ) and equilibrium adsorption capacity ( $q_e$ , μg/g) were calculated using Equation 1 and Equation 2, respectively:<sup>13</sup>

$$q_t = V \frac{C_o - C_t}{m} \quad \text{Equation 1}$$

$$q_e = V \frac{C_o - C_e}{m} \quad \text{Equation 2}$$

where  $V$  is the solution volume (L);  $m$  is the weight of the adsorbent (g);  $C_o$ ,  $C_t$  and  $C_e$  (μg/L) are the concentrations of the adsorbate at the initial, certain and equilibrium times.

To better understand the factors and mechanisms controlling the adsorption of MC-LR onto ChMWCNT, the experimental data obtained at various contact times were fitted into kinetics models namely, pseudo first order (PFO) and pseudo second order (PSO) and the Weber–Morris intra-particle diffusion models. The mathematical expressions (nonlinear fits) of the PFO and PSO kinetic models are shown in Equations 3 and 4, respectively.<sup>14</sup>

$$q_t = q_e(1 - e^{-k_1 t}) \quad \text{Equation 3}$$

$$q_t = \frac{(k_2 q_e^2 t)}{(1 + k_2 q_e t)} \quad \text{Equation 4}$$

where  $q_t$  (mg/g) and  $q_e$  (mg/g) are the amounts of MC-LR adsorbed at time  $t$  (h) and equilibrium, respectively, and  $k_1$  (1/h) and  $k_2$  (g/mg.h) are the PFO and PSO adsorption rate constants, respectively.

Equation 5 shows the Weber–Morris intra-particle diffusion model:

$$q_t = k_{id} t^{1/2} + C \quad \text{Equation 5}$$

where  $k_{id}$  is the intra-particle diffusion coefficient (mg/g. min<sup>1/2</sup>), and  $C$  (g/g) a constant associated with diffusion resistance

Adsorption isotherm models, namely, Langmuir and Freundlich adsorption isotherm models, were used to give more insight into the relationship between the adsorbate concentration and the solid phases in the aqueous solution at equilibrium.<sup>15</sup> The nonlinear mathematical expressions of the Langmuir and Freundlich isotherm models are shown in Equation 6 and Equation 7, respectively.<sup>14</sup>

$$q_e = \frac{Q_{max} K_L C_e}{1 + K_L C_e} \quad \text{Equation 6}$$

$$q_e = K_f C_e^{\frac{1}{n}} \quad \text{Equation 7}$$

where  $Q_{max}$  (mg/g) and  $K_L$  (L/mg) are the maximum adsorption capacity of the adsorbent and the Langmuir constant related to the adsorption energy of the adsorbent, respectively.  $K_f$  (mg/g (mg/L)<sup>-1/n</sup>) and  $n$  (-) are the Freundlich constant and adsorption strength, respectively.

For the Langmuir isotherm, the adsorption process efficiency was determined using a dimensionless constant separation factor  $R_L$ , calculated using the calculated  $K_L$  from Equation 6 as follows (Equation 8):

$$R_L = \frac{1}{1 + K_L * C_e} \quad \text{Equation 8}$$

If the  $R_L$  values are found to be between 0 and 1, then the process of adsorption is deemed favourable at the temperatures studied.<sup>15</sup>

### Desorption optimisation

Supernatants were discarded after adsorption equilibration was achieved (based on optimum equilibration time and dosage in sections on optimisation of equilibration time; optimisation of dosage and adsorption and equilibrium studies). The residual adsorbent was extracted with varying percentages of methanol (0%, 20%, 50%, 80% and 100%) through sonication (SCIENTEC Ultrasonic Cleaner, Model 705, South Africa) for 5 min to release toxins before centrifugation at 570 rcf for 10 min. The whole cycle of sonication and centrifuging was repeated three times and the supernatant pooled to give approximately a 15-mL extract of each sample. The pooled samples were then evaporated to dryness under a gentle stream of nitrogen ( $N_2$ ) gas, with the residue suspended in 1 mL of Milli-Q water followed by analysis using the ELISA method.

### Adsorption and desorption in SPATT bag format

#### SPATT construction and activation

SPATT bags were constructed from nylon mesh with approximately 95–100  $\mu$ m pore size. The nylon mesh was sewn on three sides using a sewing machine and the bag was filled with 0.2 g of the ChMWCNT composite, then the fourth side was sewn to form a finished SPATT bag of approximately 60  $\times$  60 mm dimension. The SPATT bags were activated by soaking in 100% methanol (MeOH) for 48 h, then rinsed thoroughly in Milli-Q water for removal of any MeOH residues and kept in Milli-Q water at 4–6 °C before use.

#### Adsorption experiment with field water

Raw dam water collected from Roodeplaait Dam was used for the SPATT adsorption experiment with field water. Before the experiment, the raw dam water was analysed for pH, total dissolved solids (TDS), electrical conductivity (EC) and turbidity. TDS, pH and EC were determined using a Jenway pH/Cond meter model (430), and turbidity was determined using a TB200 portable turbidity meter model (#TB200-10). The raw dam water (1 L) was placed in 1 L amber bottles, and the SPATT bags packed with 0.2 g of ChMWCNT were introduced to each bottle and the solutions were shaken at 145 rpm for 30 min at room temperature. The SPATT bags were removed after 30 min, rinsed in Milli-Q water and kept at 4–6 °C before extraction.

#### SPATT extraction

The SPATT bags were oven dried at 40 °C, then cut open and the material was placed in 15 mL centrifuge tubes. The toxins were extracted using 100% MeOH through sonication (5 min) to release toxins and centrifuged at 1750 rpm as described under 'Desorption optimisation'. The pooled supernatant was collected and dried at 50 °C under a stream of nitrogen.

The dried material was then reconstituted with 1 mL of Milli-Q water and analysed using the ELISA method (ELISA test kits), EUROFINS (Kit Lot No: 19I1120: PN 520011) and liquid chromatography–mass spectrometry (LC–MS).

#### Determination of MC levels in the residues and extracted material

EUROFINS microcystin/nodularin ELISA plate kit were used for the analysis of total MCs in the samples following the manufacturers' instructions. The method is based on a direct competitive ELISA for quantitative detection of MCs and nodularins on the polyclonal antibodies. To determine the levels of some of the congeners of MCs (LR, RR and YR) adsorbed by the composites, a chromatographic method using a Shimadzu triple quadrupole LC–MS/MS system (model LCMS-8045, Shimadzu Corporation, Japan) was used.

#### Chromatographic conditions

Levels of microcystins (LR, RR and YR) in the samples were determined on a triple quadrupole LC–MS/MS system (model LCMS-8045, Shimadzu Corporation, Japan) with a Shim-pack Velox SP-C18, 2.7  $\mu$ m, with dimensions 2.1  $\times$  100 mm (Shimadzu, Japan). The injection volume was set at 10  $\mu$ L and the mobile phases used were 0.1% formic acid (FA) in water (A) and 0.1% FA in acetonitrile (B). A flow rate of 0.5 mL/min and a 5-min binary gradient were used with an elution profile of 2% B (0.4 min), linear gradient to 70% B (3.1 min), 100% B (0.5 min), and, finally, 2% B (1 min). Detection limits were 0.5  $\mu$ g/L for all the three MC congeners used.

The final concentration of the toxins in the samples was determined by using Equation 9:

$$\text{Conc in sample } (\mu\text{g/L}) = \left( \frac{C_o \times \text{Vol of extract used (L)}}{\text{Volume of sample used (L)}} \right) \quad \text{Equation 9}$$

where  $C_o$  = the concentration of the sample determined from the calibration curve ( $\mu$ g/L)

To determine the microcystin concentrations adsorbed to the SPATT composite/resin, Equation 10 was used:

$$\mu\text{g/g (resin)} = \frac{(\mu\text{g/L in extract} \times 0.001 \text{ L extract vol})}{0.2 \text{ g (composite)}} \quad \text{Equation 10}$$

where the extract volume is 0.001 L and is 0.2 g of ChMWCNT.

To compare the levels of MCs adsorbed and desorbed by different adsorbents and solutions, analysis of variance (ANOVA) and/or the Kruskal–Wallis tests were used at 95% confidence interval (CI) using GraphPad InStat 3 (GraphPad Software, California, USA).

## Results and discussion

### Physicochemical characterisation

#### Fourier transform infrared analysis

The FTIR spectra for raw chitosan, ChGLA and ChMWCNT composite are shown in Figure 1. The notable peaks of chitosan can be attributed to: the broad and strong band ranging from 3200 to 3600/cm corresponds to the presence of –OH and –NH<sub>2</sub> groups, 2927/cm (CH<sub>2</sub> symmetric stretch), 1634/cm (C = O stretching vibration), 1154/cm (C–O–C bending vibration), and 1066/cm (C–OH stretching vibration) as also observed by Li et al.<sup>16</sup> Major differences in the spectra of chitosan compared to ChGLA and ChMWCNT were the presence of C–O–C band at 1154/cm in chitosan but not in the two crosslinked products and the presence of the amide II at 1554/cm in the crosslinked material (ChGLA and ChMWCNT) but not in the spectra of chitosan (Figure 1). Of importance to note were the broader peaks of the ChMWCNT compared to the other two materials, which probably indicated the coating of the chitosan by the multi-walled carbon nanotubes as was also observed by Liu et al.<sup>17</sup>

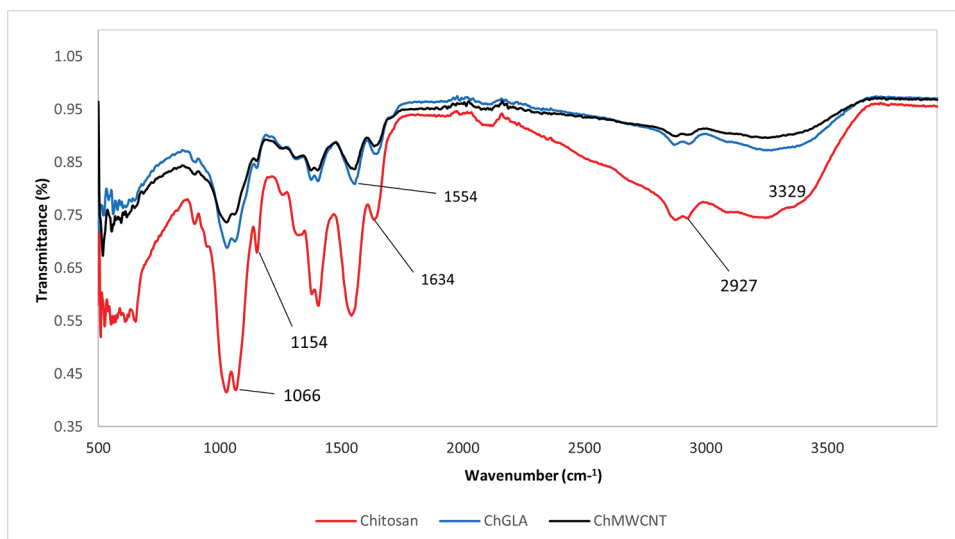


**Figure 1:** FTIR spectra for chitosan, ChGLA and ChMWCNT.

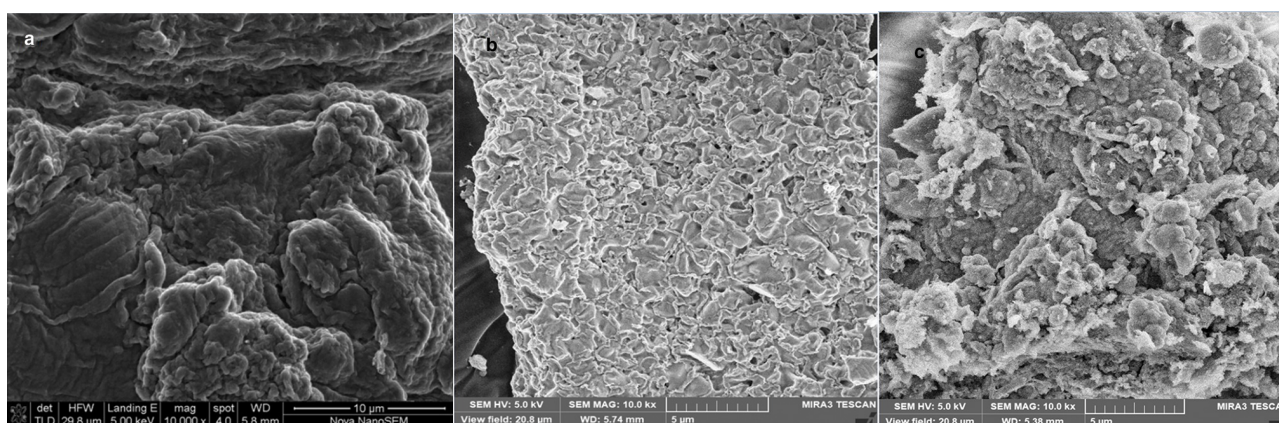


**Figure 2:** SEM images for (a) raw chitosan, (b) ChMWCNT before adsorption and (c) ChMWCNT after adsorption x10 000 magnification.

### Morphological analysis

Figure 2a shows the surface morphology of raw chitosan at x10 000 magnification. The SEM images show a slightly rough and dense surface with large clusters of particles for raw chitosan. After the crosslinking and introduction of multi-walled CNTs (Figure 2b), the surface structure appears more porous and flaky. The introduction of multi-walled CNTs seems to have enhanced pore formation. A clear distinction of the ChMWCNT morphology before and after adsorbing MCs can be seen in Figure 2b vs 2c with the structure becoming deformed and irregular upon adsorption. Figure 2c shows the formation of granules in the used material, which could be attributed to the swelling of the material during adsorption with the pores appearing saturated after use.

### Surface area, pore volume and pore size

Specific surface area and pore volume are very important aspects for any material to be used for the adsorption of MCs, as MCs are large molecules and cannot easily enter into the micropores of materials with low micropore sizes.<sup>1</sup> Table 1 shows the surface area and pore size of the raw chitosan, synthesised ChGLA, ChMWCNT and the Diaion® HP-20 resin, which were evaluated using the Brunauer–Emmett–Teller (BET) method.

The results indicate that the Diaion® HP-20 resin had surface area, pore volume and pore size comparable to what was reported by Li et al.<sup>18</sup> In terms of the surface area, pore volume and pore size of the synthesised materials, raw chitosan had the lowest, followed by ChGLA, ChMWCNT. The Diaion® HP-20 resin displayed far more superior surface area and pore volume compared to any of the synthesised material, but the ChMWCNT had much greater pore sizes compared to Diaion® HP-20.

Introduction of multi-walled CNTs onto the ChGLA, improved the surface area, pore volume and pore size of the chitosan, and hence ChMWCNT seemed more suitable for the adsorption of MCs compared to ChGLA. Regardless of the lower surface area of the ChMWCNT compared to Diaion® HP-20, its higher pore sizes make it ideal for the adsorption of MCs. Li et al.<sup>18</sup> reiterate the importance of materials' pore size instead of surface area in determining the equilibration rates and abilities to adsorb the toxins.

### Adsorption and desorption characteristics of the composite for microcystins

Results of batch adsorption experiments showing the effects of the effect of contact time, initial adsorbate (MC-LR) concentration and adsorbent (ChMWCNT) dosage are presented in Figure 3a, b and c, respectively.

#### Effect of contact time

The effect of contact time was evaluated to establish the equilibrium time for optimum adsorption of MC-LR onto ChMWCNT and establish the adsorption kinetics. The results in Figure 3a show that MC-LR was rapidly adsorbed in the first 15 min of the reaction and then slowed down as the reaction time increased to 30 min where optimum uptake of MC-LR was recorded. Thereafter, removal efficiency remained almost constant as the time increased to 60 min indicating that equilibrium had been reached.

The rapid adsorption of MC-LR in the initial stages (5–15 min) of contact could be attributed to binding of adsorbate onto the readily available active sites on the outer surface of the ChMWCNT. In the early stages, there are many

**Table 1:** Surface area, pore volume and pore size of HP20, ChGLA\*, ChMWCNT and Chitosan

	HP20	ChGLA	ChMWCNT	Chitosan
<b>Surface area (m<sup>2</sup>/g)</b>				
Single point surface area	618.0379	1.7616	8.0174	0.264
BET surface area	653.6041	1.8978	8.377	0.3241
BJH adsorption cumulative surface area of pores	481.58	0.506	8.424	0.158
BJH desorption cumulative surface area of pores	475.1997	0.49	10.5357	0.9885
<b>Pore volume (cm<sup>3</sup>/g)</b>				
Single point adsorption total pore volume of pores	0.74539	–	0.02248	–
BJH adsorption cumulative volume of pores	0.999586	0.00022	0.029747	0.001056
BJH desorption cumulative volume of pores	0.983416	–	0.029914	0.001138
<b>Pore size (Å)</b>				
Adsorption average pore width (4V/A by BET)	45.6172	–	107.3432	–
BJH adsorption average pore diameter (4V/A)	83.026	17.397	141.254	267.817
BJH desorption average pore diameter (4V/A)	82.779	–	113.57	46.043

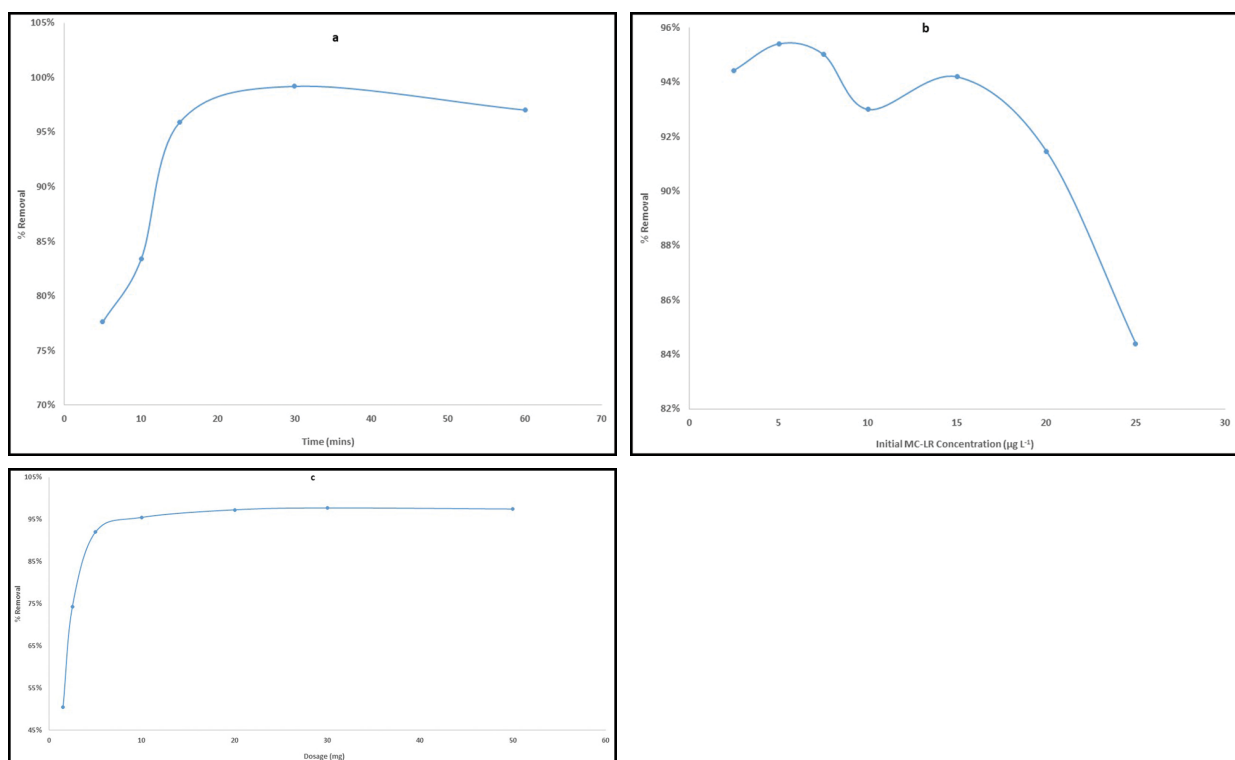


**Figure 3:** (a) Effect of contact time on the adsorption of MC-LR onto ChMWCNT. (b) Adsorption of MC-LR onto ChMWCNT as a function of initial concentration (5 µg/L initial concentration, 10 mg/5 mL adsorbent dosage). (c) Adsorption of MC-LR onto ChMWCNT as a function of adsorbent (pH 6.5 ± 0.5 and shaking speed of 145 rpm).

sorption sites available for occupation by the adsorbate, thus higher initial rates; then as the reaction continues, the sorption sites and concentration of the adsorbate decreases and the rate of adsorption also lowers.<sup>14</sup>

Based on that, 30 min was adopted as the reaction time for subsequent experiments. Our findings were similar to those of Zhao et al.<sup>1</sup> who found the equilibration times of MCs onto the Diaion® HP-20 resin to be 30 min, but that of SP700 to be 15 min. This implies that the synthesised composite adsorbs MCs at comparable rate with other adsorbents being used for the same purpose.

To further explain the adsorption mechanisms and the adsorption rate controlling factors, the experimental data were fit into reaction kinetics models namely PFO, PSO and intra-particle diffusion.<sup>19</sup> The nonlinear plot for PFO and PSO are presented in Figure 4a whilst the constant parameters are presented in Table 2. The PSO models showed a higher correlation coefficient ( $R^2 = 0.875$ ); this means that the experimental data are better explained by the PSO model, thus showing that the adsorption was occurring through chemisorption. In a related study locally, Mashile et al.<sup>20</sup> also found their adsorption data to be fitting the fitted the

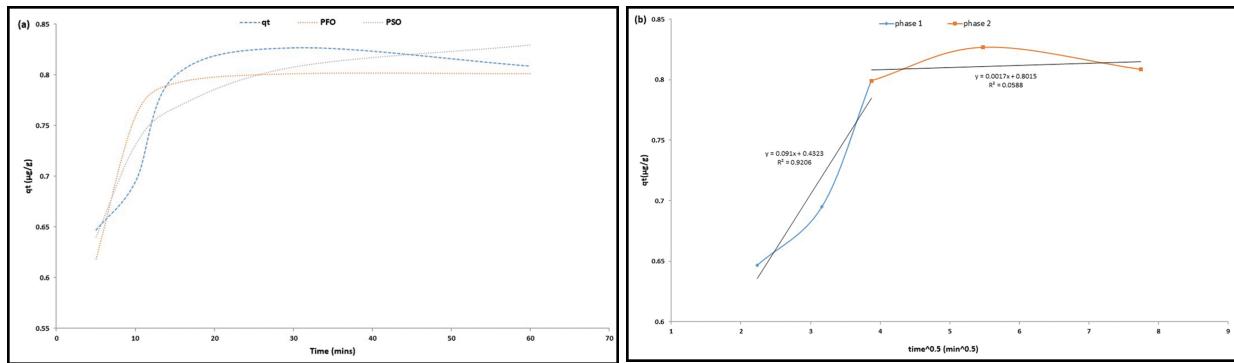


**Figure 4:** (a) Results of kinetics experiment on ChMWCNT and nonlinear regression analysis of PFO and PSO models. (b) Intra-particle diffusion of MC-LR onto ChMWCNT (initial MC-LR concentration: 5 µg/L, adsorbent dose: 30 mg/5 mL, time: 5, 10, 15, 30 and 60 min).

**Table 2:** Parameters of pseudo-first-order and second-order reaction kinetics

	Concentration (µg/L)	Pseudo-first-order model			Pseudo-second-order model		
		$q_e$ (µg/g)	$K$ (L/mg)	$R^2$	$q_e$ (µg/g)	$K$ (L/mg)	$R^2$
<b>ChMWCNT</b>	5	0.801	0.295	0.773	0.852	0.710	0.875

pseudo-second-order model when applying tyre-based activated carbon for the removal of MC-LR via adsorption. The adsorption mechanism of MC-LR onto the composite can be explained in terms of the functional groups in chitosan. Chitosan has numerous amino ligands and hydroxyl groups on its surface,<sup>21</sup> which are all considered to be active sites for the sorption of MCs.

The experimental data were also fitted into intra-particle diffusion plot to understand the rate controlling factors limiting the adsorption of MC-LR onto ChMWCNT (Figure 4b). Based on this model, if a graph/plot displays multi-linearity, this is an indication that there are more than one adsorption processes taking place and the rate-limiting step is not the intra-particle diffusion.<sup>22</sup> In this study, a multi-linear plot was obtained (Figure 4b) thus showing a two-step diffusion process. Figure 4b shows a sharp first step (in the first 15 min) showing external mass transfer through instantaneous sorption. The second and last step (the equilibrium stage) shows intra-particle diffusion and a plateau demonstrating slow diffusion as the levels of the adsorbate decrease. These findings thus show that the adsorption of MC-LR onto ChMWCNT is not solely controlled by intra-particle diffusion. Similar findings were also reported by Mashile et al.<sup>20</sup> who also found that the adsorption of MC-LR onto tyre-based activated carbon was not controlled by intra-particle diffusion as the sole rate-determining step.

**Effect of adsorbent dosage**

Dosage of adsorbent is known to have an effect on removal efficiency of adsorbates because increasing the adsorbent dosage increases the available active sites for adsorption. Findings in Figure 3c show that the adsorption of MC-LR onto ChMWCNT was increasing with increasing dose of the adsorbent. This is because increasing the dosage of the adsorbent increased the active sites for the MC-LR to be adsorbed thus an increase in removal efficiency. Maximum adsorption was reported to be 97% at a dose of 30 mg per 5 mL of the solution, and this was adopted as the optimum dose and used in the subsequent experiments.

**Effect of adsorbate concentration**

The adsorbates' initial concentration has a direct effect on the rate of adsorption, and this makes it a parameter of paramount importance to investigate to understand the adsorption process. The effect of initial concentration on the adsorption of MC-LR by ChMWCNT was evaluated using seven initial solution concentrations of MC-LR (2.5, 5, 7.5, 10, 15, 20 and 25 µg/L) and a dosage of 30 mg per 5 mL solution. Results in Figure 3b show that the removal efficiency (as % removal) of MC-LR was declining as the concentration of the adsorbate was increased. The trend observed is due to adsorbent's active site being exhausted by the adsorbate with an increase in the initial MC-LR concentrations. Highest MC-LR removal was

reported when a 5 µg/L solution was used. This was then selected as the optimum concentration in the subsequent experiments.

The adsorption data obtained when investigating the effect of the adsorbate initial concentration on the process were fitted into nonlinear equations of Langmuir and Freundlich isotherm models. Analysis of the equilibrium isotherms gives data on the adsorption capacity, which is crucial when investigating adsorption systems.<sup>14</sup> The Langmuir model assumes that the adsorption process happens on a homogenous surface with a single layer adsorption taking place at all the available adsorption sites. The model also assumes no interaction between the adsorbent and the adsorbate.<sup>22</sup> On the other hand, the Freundlich model assumes that adsorption occurs in a multi-layer on a heterogeneous adsorbent. The isotherm model assumes adsorption sites to be having unequal energy which differs exponentially, and this results in numerous adsorbate layers forming onto the surface of the adsorbent.<sup>19</sup>

The nonlinear plots for Langmuir and Freundlich isotherms are shown in Figure 5 and their respective constant parameters are shown in Table 3. Based on the correlation coefficient values ( $R^2$ ) (Table 3), the data better fitted the Langmuir isotherm model, thus inferring a monolayer uniform adsorption onto the surface of the ChMWCNT composite and no interaction of the adsorbate molecules.

The calculated  $R_L$  (dimensionless equilibrium parameter) values for the Langmuir isotherm and the Freundlich adsorption intensity ( $1/n$ ) in Table 3 were all between 0 and 1, thus showing that the adsorption of MC-LR onto the ChMWCNT composite is favourable. However, when compared to the adsorption capacities of other adsorbents applied in SPATT for microcystins as reported by Zhao et al.<sup>1</sup> (Table 4), the adsorption capacities of Diaion® HP-20 and SEPABEADS SP700 were found to be much higher than the developed composite. Even though superior adsorption capacities were observed by Zhao et al.<sup>1</sup> for the resins Diaion® HP-20 and SEPABEADS SP700, the huge differences with the developed composite could also be due to the huge differences in the experimental conditions, with Zhao et al.<sup>1</sup> having used microcystin concentrations (MC-LR 1 980–1.488 6 × 10<sup>5</sup> µg/L) which were at least a thousand times more and adsorbent dosages (0.1 g) which were at least three times more than applied in this study.

**Desorption study on ChMWCNT composite**

The desorption of MC-LR from the ChMWCNT composite was tested in five different aqueous MeOH solutions (0%, 20%, 50%, 80% and 100%). Recoveries of MC-LR from the composite using these solutions are shown in Figure 6. Pure water (0%), 20% and 50% MeOH solutions proved to be very ineffective in desorbing MC-LR. Higher mean recoveries of 71.99 ± 4.47% and 84.71 ± 6.47% were observed for

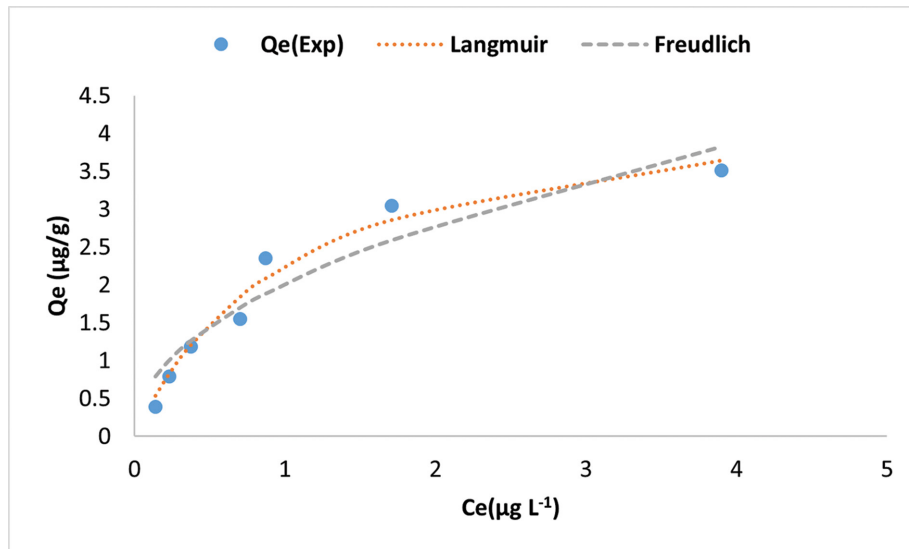


Figure 5: Adsorption equilibrium isotherms for MC-LR on ChMWCNT.

Table 3: Parameters of Langmuir’s and Freundlich’s isotherm models at 25 °C

	Langmuir’s isotherm model			Freundlich’s isotherm model		
	$Q_{max}$ (µg/g)	$K_L$ (L/mg)	$R^2$	$K_F$ (L/mg)	$1/n$	$R^2$
ChMWCNT	4.639	0.938	0.972	2.012	0.473	0.908

Table 4: List of adsorbents used in SPATT for microcystins

Adsorbent	Type of microcystin	Adsorption capacity (µg/g)	Reference
HP20	MC-LR	335	Zhao et al. <sup>1</sup>
SP700	MC-LR	828	Zhao et al. <sup>1</sup>
ChMWCNT	MC-LR	4.639	This study

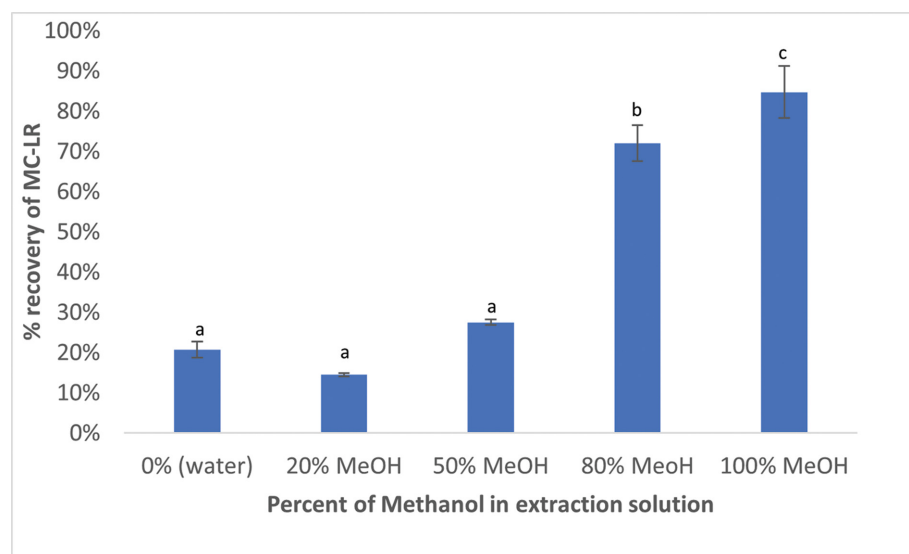


Figure 6: Desorption efficiency of MC-LR from ChMWCNT using various percentages of methanol as the extraction solution. Data labelled with different small letters (a, b, c) differed significantly at  $p < 0.05$  in each bar ( $n = 3$ ).

80% and 100% MeOH, respectively. Similar findings were reported by Zhao et al.<sup>1</sup> who reported the highest recovery of  $78.1 \pm 4.1\%$  for MC-LR from the resin SEPABEADS SP700 using 100% MeOH. However, Zhao et al.<sup>1</sup> found better recoveries of  $91.5 \pm 4.6\%$  for MC-LR with 75% MeOH compared to 100% methanol ( $\pm 78\%$  recovery).

Such findings imply that, compared to Diaion® HP-20, the synthesised composite has a stronger affinity for MC-LR. However, the fact that some MCs were desorbed when 100% water was used suggests a possibility of MCs leaching from the composite in solution when this material is used for SPATT.

#### Application in raw dam water and SPATT bag format

To determine the potential of the composite to adsorb and desorb different congeners of MCs (MC-LR, RR and YR), we exposed SPATT samplers loaded with 0.2 g of the composite to 1 L of raw dam water with pH of  $7.29 \pm 0.71$ , EC of  $878.67 \pm 42.44 \mu\text{S/cm}$  and MCs with the following mean concentrations: MC-LR  $25.14 \pm 2.34$ ; MC-YR  $10.21 \pm 0.41$  and MC-RR  $7.92 \pm 0.10 \mu\text{g/L}$ . Similar congeners (MC-LR, -YR and -RR), were reported by Pedro et al.<sup>23</sup> when using passive sampling devices (PSDs) followed by LC-MS when monitoring the toxins in Southern Mozambique. Levels of MCs in the range 2.1–159.4 ng/g of PSDs reported by (23) were consistent to the levels reported here (Figure 7).

The findings in Figure 7a and 7b show that except for MC-YR, where the recovery seemed disproportional to the levels in solution, the levels of

MC-LR and MC-RR recovered were representative/proportional to the levels in the dam water. This seems to imply less affinity or recoveries of MC-YR compared to the other two congeners monitored. Such findings are consistent with Cook and Newcombe<sup>24</sup> who found the adsorption of different MC congeners in the order MC-RR > MC-YR > MC-LR > MC-LA, when investigating the performance of charcoal and wood powdered activated carbons (PACs) using the surface diffusion model. Similar adsorption performances MC-RR > MC-YR > MC-LR > MC-LA were also reported by Ho et al.<sup>25</sup> for adsorption behaviours of PACs. It is also highly possible that the water had other congeners of MCs not monitored here as reported by Mbukwa et al.<sup>26</sup> for the same catchment, which could have outcompeted MC-YR for adsorption sites onto the composite.

#### Conclusions

In this study, a glutaraldehyde-crosslinked chitosan-multi-walled carbon nanotube (ChMWCNT) composite was synthesised and evaluated for its adsorption and desorption of MC-LR in batch experiments and then later applied in raw dam water to assess its applicability in the passive sampling of MCs in SPATT samplers. The optimum conditions for MC-LR adsorption were 30 min contact time,  $5 \mu\text{g/L}$  dosage and 30 mg per 5 mL dosage at ambient room temperatures and natural pH water. The composite was found to be efficient in adsorbing MC-LR, with up to 97% removal of the toxin under optimised conditions. The kinetics data for the adsorption were better explained by the pseudo-second-order model, meaning that the adsorption

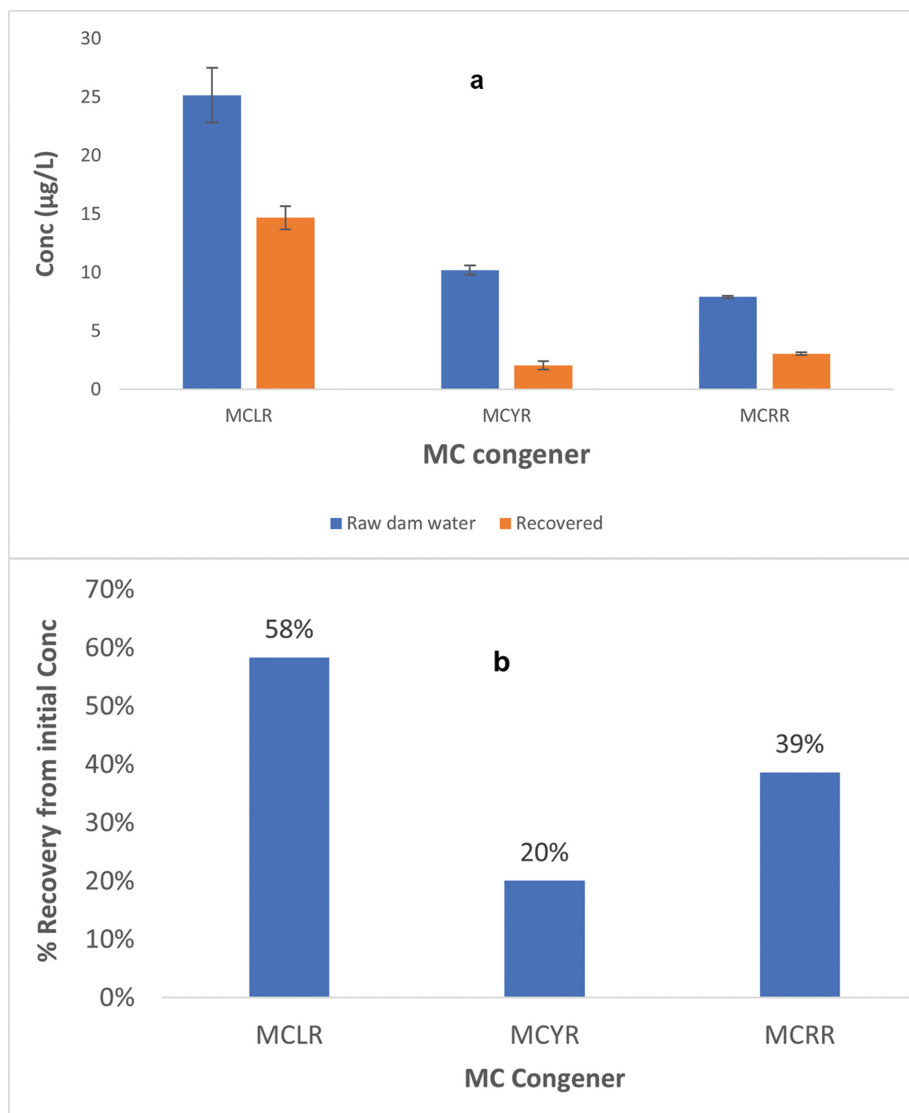


**Figure 7:** (a) The different levels of MCs (LR, YR, RR) adsorbed onto ChMWCNT. (b) Percentage Levels of MC (LR, YR, RR) adsorbed from the raw dam water.



was occurring through chemisorption. The experimental data were fitting better into the Langmuir isotherm compared to the Freundlich isotherm, thus inferring a monolayer surface adsorption of MC-LR onto ChMWCNT. Adsorption capacity of 4.639 µg/g was reported, and  $R_L$  (dimensionless equilibrium parameter) values for the Langmuir isotherm were between 0 and 1, inferring that adsorption of MC-LR onto the ChMWCNT composite is favourable. In terms of desorption, 100% methanol was found to be most effective with a highest mean desorption efficiency of  $84.71 \pm 6.47\%$  reported. When applied for the adsorption in raw dam water, the composite was saturated within 2 days of exposure and adsorbed and desorbed the three congeners of MCs (-LR, -RR and -YR) relatively well. Based on the findings, we recommend further studies looking into the effect of other parameters such as pH, effect of co-existing pollutants and ions and field SPATT monitoring of MCs using the developed composite to assess its performance on different cyanotoxins. The results show that the chitosan-based composite, which can be derived from the deacetylation of chitin from seafood waste, which is abundant in South Africa, can be a cheaper ingredient for a sorbent to be used in the SPATT for microcystins in water bodies used for drinking water and agricultural purposes.

## Acknowledgements

We acknowledge the Department of Nutrition (Faculty of Health Sciences) at the University of Venda for the use of the Shimadzu High-Performance Liquid Chromatography Triple Quadrupole Mass Spectrometer (LCMS-8045). Funding for this study was granted by the South African Water Research Commission (WRC) Project No: K5/2972.

## Competing interests

We have no competing interests to declare.

## Authors' contributions

G.P.K.: Conceptualisation, methodology, data curation, writing – the initial draft and revisions. M.W.G.: Conceptualisation, validation, student supervision, funding acquisition, writing – revisions. N.E.M.: Data curation, writing – revisions.

## References

- Zhao H, Qiu J, Fan H, Li A. Mechanism and application of solid phase adsorption toxin tracking for monitoring microcystins. *J Chromatogr A*. 2013;1300:159–164. <http://dx.doi.org/10.1016/j.chroma.2013.02.048>
- Díez-Quijada L, Guzmán-Guillén R, Prieto Ortega AI, Llana-Ruiz-Cabello M, Campos A, Vasconcelos V, et al. New method for simultaneous determination of microcystins and cylindrospermopsin in vegetable matrices by SPE-UPLC-MS/MS. *Toxins (Basel)*. 2018;10(10):1–16. <https://doi.org/10.3390/toxins10100406>
- Howard MDA, Nagoda C, Kudela RM, Hayashi K, Tatters A, Caron DA, et al. Microcystin prevalence throughout lentic waterbodies in coastal southern California. *Toxins (Basel)*. 2017;9(7):1–21. <https://doi.org/10.3390/toxins9070231>
- Buratti FM, Manganelli M, Vichi S, Stefanelli M, Scardala S, Testai E, et al. Cyanotoxins: Producing organisms, occurrence, toxicity, mechanism of action and human health toxicological risk evaluation. *Arch Toxicol*. 2017;91(3):1049–1130. <https://doi.org/10.1007/s00204-016-1913-6>
- Pedro O, Correia D. Occurrence of microcystins in freshwater bodies in Southern Mozambique. *J Res Environ Sci Toxicol*. 2012;1(14):58–65. <http://www.interestjournals.org/articles/occurrence-of-microcystins-in-freshwater-bodies-in-southern-mozambique.pdf>
- Wood SA, Holland PT, MacKenzie L. Development of solid phase adsorption toxin tracking (SPATT) for monitoring anatoxin-a and homoanatoxin-a in river water. *Chemosphere*. 2011;82(6):888–894. <http://dx.doi.org/10.1016/j.chemosphere.2010.10.055>
- MacKenzie L, Beuzenberg V, Holland P, McNabb P, Selwood A. Solid phase adsorption toxin tracking (SPATT): A new monitoring tool that simulates the biotoxin contamination of filter feeding bivalves. *Toxicon*. 2004;44(8):901–918. <https://doi.org/10.1016/j.toxicon.2004.08.020>
- Zendong Z, Herrenknecht C, Abadie E, Brissard C, Tixier C, Mondeguer F, et al. Extended evaluation of polymeric and lipophilic sorbents for passive sampling of marine toxins. *Toxicon*. 2014;91:57–68. <http://dx.doi.org/10.1016/j.toxicon.2014.03.010>
- Gomez-Maldonado D, Filpponen I, Vega Erramuspe IB, Johansson L, Mori MF, Jayachandra Babu R, et al. Development of a  $\beta$ -cyclodextrin-chitosan polymer as active coating for cellulosic surfaces and capturing of microcystin-LR. *Surf Interfaces*. 2022;33:102192. <https://doi.org/10.1016/j.surfint.2022.102192>
- Tran QN, Jin X, Doan NQH. Enhanced removal of extracellular microcystin-LR using chitosan coagulation-ultrafiltration: Performance and mechanisms. *J Environ Chem Eng*. 2022;10(3):107902. <https://doi.org/10.1016/j.jece.2022.107902>
- Gonçalves JO, Santos JP, Rios EC, Crispim MM, Dotto GL, Pinto LAA. Development of chitosan based hybrid hydrogels for dyes removal from aqueous binary system. *J Mol Liq*. 2017;225:265–270. <http://dx.doi.org/10.1016/j.molliq.2016.11.067>
- Alves DCS, Gonçalves JO, Coseglio BB, Burgo TAL, Dotto GL, Pinto LAA, et al. Adsorption of phenol onto chitosan hydrogel scaffold modified with carbon nanotubes. *J Environ Chem Eng*. 2019;7(6). <https://doi.org/10.1016/j.jece.2019.103460>
- Lim DT, Tuyen TN, Nhiem DN, Duc DH, Chuc PN, Bac NQ, et al. Fluoride and arsenite removal by adsorption on  $\text{La}_2\text{O}_3$ -CeO<sub>2</sub>/laterite. *J Nanomater*. 2021;2021. <https://doi.org/10.1155/2021/9991050>
- Choi M, Lee C. Enhanced uric acid adsorption on aluminum-impregnated kenaf biochar: Adsorption characteristics and mechanism [preprint]. *Res Square*. 2022; version 1. <https://doi.org/10.21203/rs.3.rs-1504419/v1>
- Braik S, Amor TB, Michelin L, Rigolet S, Bonne M, Lebeau B, et al. Natural water defluoridation by adsorption on Laponite clay. *Water Sci Technol*. 2022;85(6):1701–1719. <https://doi.org/10.2166/wst.2022.091>
- Li B, Shan CL, Zhou Q, Fang Y, Wang YL, Xu F, et al. Synthesis, characterization, and antibacterial activity of cross-linked chitosan-glutaraldehyde. *Mar Drugs*. 2013;11(5):1534–1552. <https://doi.org/10.3390/md11051534>
- Liu AH, Sun KN, Li AM. Preparation of chitosan/carbon nanotubes composites. *Adv Compos Lett*. 2007;16(4):143–148. <https://journals.sagepub.com/doi/pdf/10.1177/096369350701600403>
- Li A, Ma F, Song X, Yu R. Dynamic adsorption of diarrhetic shellfish poisoning (DSP) toxins in passive sampling relates to pore size distribution of aromatic adsorbent. *J Chromatogr A*. 2011;1218(11):1437–1442. <http://dx.doi.org/10.1016/j.chroma.2011.01.043>
- Mudzielwana R, Gitari WM, Ndungu P. Evaluation of the adsorptive properties of locally available alumino-silicate clay in As(III) and As(V) remediation from groundwater. *Phys Chem Earth*. 2019;112(2018):28–35. <https://doi.org/10.1016/j.pce.2018.11.008>
- Mashile PP, Mpupa A, Nomngongo PN. Toxin adsorptive removal of microcystin-LR from surface and wastewater using tyre-based powdered activated carbon: Kinetics and isotherms. *Toxicon*. 2018;145:25–31. <https://doi.org/10.1016/j.toxicon.2018.02.044>
- Sanford S, Singh KS, Chai S, LeClair G. Study of natural adsorbent chitosan and derivatives for the removal of caffeine from water. *Water Qual Res J Canada*. 2012;47(1):80–90. <https://doi.org/10.2166/wqrjc.2012.021>
- Zaidi R, Khan SU, Farooqi IH, Azam A. Investigation of kinetics and adsorption isotherm for fluoride removal from aqueous solutions using mesoporous cerium-aluminum binary oxide nanomaterials. *RSC Adv*. 2021;11(46):28744–28760. <https://doi.org/10.1039/d1ra00598g>
- Pedro O, Correia D, Lie E, Skåre JU, Leão J, Sandvik M, et al. Polymerase chain reaction (PCR) detection of the predominant microcystin-producing genotype of cyanobacteria in Mozambican lakes. *Afr J Biotechnol*. 2011;10(83):19299–19308. <https://doi.org/10.5897/AJB11.1521>
- Cook D, Newcombe G. Removal of microcystin variants with powdered activated carbon. *Water Supply*. 2002;2(5-6):201–207. <https://doi.org/10.2166/ws.2002.0170>
- Ho L, Lambling P, Bustamante H, Duker P, Newcombe G, Supe E. Application of powdered activated carbon for the adsorption of cylindrospermopsin and microcystin toxins from drinking water supplies. *Water Res [Internet]*. 2011;45(9):2954–2964. <http://dx.doi.org/10.1016/j.watres.2011.03.014>
- Mbukwa EA, Msagati TAM, Mamba BB. Quantitative variations of intracellular microcystin-LR, -RR and -YR in samples collected from four locations in Hartbeespoort Dam in North West Province (South Africa) during the 2010/2011 summer season. *Int J Environ Res Public Health*. 2012;9(10):3484–3505. <https://doi.org/10.3390/ijerph9103484>